

# Influence of Pressure Variation Inside the Snubber on Reciprocating Hydrogen Compression System

## 왕복동식 수소 압축 시스템에서의 스너버 내부 압력변화의 영향

M. Sq. Rahman, G. H. Lee, J. S. Woo, T. S. Utomo, H. S. Chung and H. M. Jeong  
라흐만 · 이경환 · 우주식 · 토니 · 정한식 · 정효민

(received 12 February 2008, revised 17 September 2008, accepted 14 April 2009)

**주요용어** : 수소 압축(Hydrogen Compression), 스너버(Snubber), 맥동압 감소(Pressure Pulsation Reduction), 압력 손실(Pressure Loss), 전산유체역학(CFD)

**요 약** : 본 실험에서는 왕복동식 수소 압축 시스템에서 다양한 스너버 압력변화와 스너버 효과를 조사하였다. 압력값은 실험적인 방법으로 스너버 시스템에서 각각 6군데에서 압력 값을 측정하였다. 그리고 아크릴 스너버에서의 입, 출구의 압력진폭은 FFT로 얻어진다. 맥동압 감소는 결과의 입, 출구의 진폭으로써 계산되어진다. 이는 각각의 모터 주파수 30, 40, 50Hz에서 각각 58.248%, 57.026%, 56.871%의 맥동압 감소가 일어난다. 압력 손실은 각각의 모터주파수 30, 40, 50Hz에서 0.960%, 1.533%, 1.965% 손실값이 발생한다. 수치해석은 스너버 내부 모든 구역에의 압력 정보를 보여준다. 실험과 수치해석의 결과를 비교하면 좋은 일치성을 보인다. 그렇기 때문에 수치해석으로 구한 압력 예측값은 왕복동식 수소 압축 시스템의 스너버 성능을 포함하는 다양한 수학적 식에 적용가능하다.

### 1. 서 론

Lion's share of the total energy is being used in transportation sector. Roughly 97% of all energy consumed by our cars, sport utility vehicles, vans, trucks, and airplanes is still petroleum-based<sup>1)</sup>. Combustion of fossil fuels for vehicle transportation and stationary power generation emits considerable gaseous pollutants and articulates that cause serious harms to the environment. Internationally, the situation is equally problematic. In the absence of strong government policies, the worldwide use of oil in transport will nearly double between 2000 and 2030, leading to a similar increase in greenhouse gas emissions<sup>2)</sup>. Recently, alternative fuels and alternative fuel vehicles are being searched

continuously and rapidly because of their potential to provide a zero-carbon transportation fuel. Besides, the energy capturing politics of different countries of the world increases the price of oil. These recent hikes in price of oil have also added impetus to the movement towards hydrogen and other alternative fuels<sup>3)</sup>. They have the potential to develop clean renewable hydrogen energy to improve the environmental performance. If generated from renewable energy, hydrogen becomes the crucial link in an inexhaustible global fuel cycle based on the cleanest, most abundant, natural, and elementary substances: H<sub>2</sub>, O<sub>2</sub> and H<sub>2</sub>O<sup>4)</sup>. Hydrogen is the most challenging of all alternative fuels. In integrating production planning and reactive scheduling for the optimization of a hydrogen supply network, compressor is an essential part<sup>5)</sup>. Amongst the all of compressors, reciprocating type is applied more for its higher pressure increasing capacity. Hydrogen transportation, storing and supply network utilize the reciprocating compressor. But pressure

정한식(책임저자) : 경상대학교 정밀기계공학과, 해양산업연구소

E-mail : hschung@gnu.ac.kr, Tel : 055-646-4766

라흐만, 이경환, 우주식, 토니 : 경상대학교 대학원

정효민 : 경상대학교 정밀기계공학과, 해양산업연구소

pulsation or fluctuation is inherent and is resulted from reciprocating back and forth movement of piston inside the cylinder. It gives several various problems for the equipment related to the system and acting gas in it. This should be attenuated. A pressure pulsation damper unit called "Snubber" is then introduced to reduce the pressure fluctuation<sup>6)</sup>. There is a buffer - a flat plate setting at a specific angle inside the snubber to damp the pulsation. A study to find out the effect of buffer presence in a snubber had already been conducted and it was found that snubber with buffer had better performance<sup>7)</sup>. So, the present study was taken to find out the pressure variation in the snubber and impact of snubber in the reciprocating hydrogen compression system.

## 2. Methodology

### 2.1 Experimental setup

A snubber was constructed with acrylic material having the following dimension. It had acrylic material buffer of 75 mm wide and 5 mm thickness placed inside the tube shaped unit. There were total six measuring points of pressure [Point 1, 2, 3] in the inlet side and [Point 4, 5, 6] in the outlet side of the snubber. The geometrical data of snubber is shown in Fig. 1. The inlet pipe of the snubber was connected to the compressor by small hose pipe (plastic) and outlet pipe was exposed to the atmosphere. The whole snubber system was set in a constructed steel structure so that it was fixed during the experiment. A piston-reciprocating compressor was used in this experiment and it was driven by an adjustable motor. The rotation of motor was controlled by setting desired frequency in the frequency regulator. The sensor probes were attached in the different pressure measuring points and the pressure signals were transmitted and amplified in a amplifier. Then they were recorded into a PC using data logger. The complete experimental setup for its different components was installed as in Fig. 2. The experiment was conducted by running the

compressor with setting motor frequency at 30, 40 and 50 Hz. Hydrogen gas has same characters with the atmospheric air. Especially to observe the pressure from physical approach (without considering the chemical character), pressured air can be used to represent hydrogen gas. Air and hydrogen gas have almost the same compressibility character. So, air compressor was used in this experiment.

### 2.2 Methods of pressure characteristics analysis

Motor driven reciprocating pump was used in this experiment. The rotation of motor

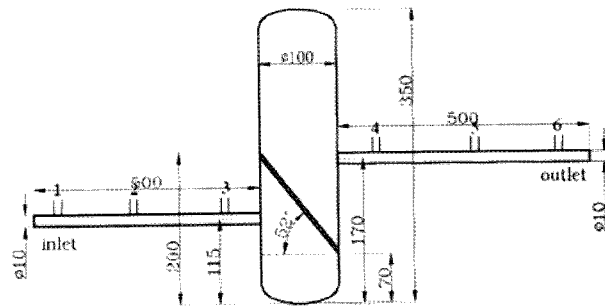


Fig. 1 Snubber dimensions with pressure measuring points

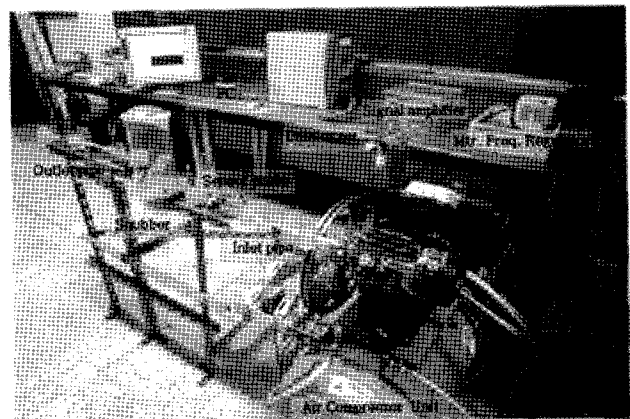


Fig. 2 Experimental set up

was controlled by its frequency regulator. The maximum motor rotation was 1800 rpm at maximum frequency(60 Hz). Relationship between compressor frequency and motor frequency were found as in equation 1.

$$f_{\text{comp}} [\text{Hz}] = f_{\text{set}} [\text{Hz}] \times 0.214 \quad (1)$$

The periodic action of propelling gas through a pipe by the to and fro movement of the piston in the cylinder in reciprocating compressor caused pulsation. The piston-crank-valve mechanism generates a variable pressure, which over time creates a composite pressure wave in the suction and discharge pipe. This composite wave is made up of a number of waves (Fig. 3). Due to periodic wave generation, multiple frequencies of pulsation are created that causes the force of vibration in the whole system.

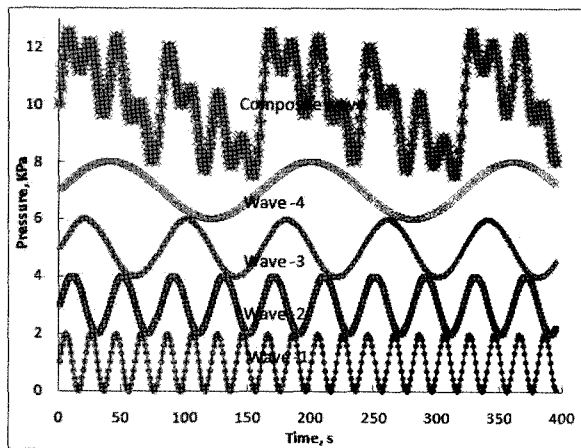


Fig. 3 Composite pressure wave generation by reciprocating piston movement in the compressor

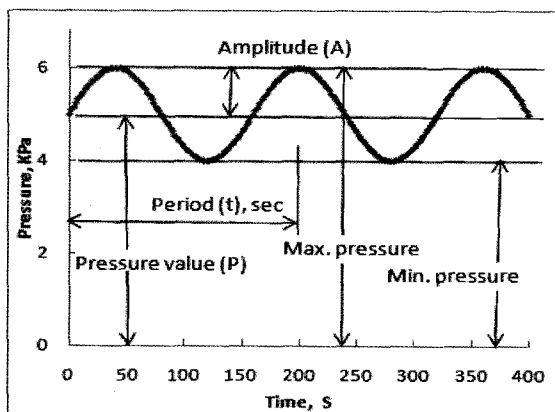


Fig. 4 Basic theory of pressure pulsation

Pressure produced by a piston in reciprocating compressor is fluctuating. Simple description of fluctuating notation is shown in Fig. 4. Pressure value and pressure amplitude can be derived as equation (2) and (3).

$$p = \frac{P_{\max} + P_{\min}}{2} \quad (2)$$

$$A = \frac{P_{\max} - P_{\min}}{2} \quad (3)$$

Same with the other gas line utilities, gas that passing through a snubber will be reduced in pressure and reduced in pressure fluctuation. It is related to the amplitude of pressure. The pressure reduction or loss and amplitude reduction can be expressed in the percentage by the equation (4) and (5), respectively.

$$P_{\text{red}}(\%) = \frac{P_{\text{in}} - P_{\text{out}}}{P_{\text{in}}} \times 100\% \quad (4)$$

$$A_{\text{red}}(\%) = \frac{A_{\text{in}} - A_{\text{out}}}{A_{\text{in}}} \times 100\% \quad (5)$$

Experimental data collected from different measuring were analyzed. Data at point 3 (input side) and point 4 (output side) were analyzed for pressure loss and amplitude reduction. The RMS values of input and output of pressure were used for pressure loss calculation. FFT analysis was done on data to find out amplitude values of the pressure waves. The resultant value of the variables was calculated by taking square root of summation of squares of all values.<sup>8)</sup> The pressure pulsation reduction was then calculated by equation (5) and pressure loss was obtained by equation (4).

### 2.3 Computational Methodology

The computational code used was Star CD (Version 3.24), which solve the full 3D time dependent Navier-Stokes, continuity and energy equations using the finite volume method. It is widely used in the numerical simulation of different flow conditions in various complex geometries and was chosen in this study because it is proven capability and validity. The turbulent flow in this investigation is considered to be transient, incompressible, viscous, Newtonian and

isotropic.

The numerical solution involves splitting the geometry into many sub-volumes and then integrating the differential equations over these volumes to produce a set of coupled algebraic equations for the velocity components, and the pressure at the centre of each volume. The solver guesses the pressure field and then solves the discretised form of the momentum equations to find new values of the pressure and velocity components. This process continues, in iterative manner, until the convergence criterion is satisfied. Turbulent model was using standard  $k-\epsilon$  model. SIMPLE algorithm revised pressure and convection term belong to Upwind Scheme. Maximum residual tolerance was set under the 0.001.<sup>9)</sup> The geometry was drawn using the CATIA (V5R15) CAD package and then imported to pro-Surf (Star CD's surface mesh generator) as an Initial Graphics Exchange Specification file (IGES). The computational mesh consists of 50,000 trimmed hexahedral cells. Inlet and outlet boundary conditions of snubber for CFD were applying the measured pressure from the experiment using pressure sensors at inlet [Point 1] and outlet [Point 6] for CFD. The model was built in a half type for the symmetrical shape of the snubber and the symmetry boundary condition was applied.

### 3. Result And Discussion

#### 3.1 Pressure and amplitude analysis

Data obtained from the experiment show pressure characteristic of gas. Shown in Fig.5 is a distribution of pressure at different points of a snubber for 3 different motor frequency [30, 40 and 50 Hz]. Along the snubber, six measuring points from input and output side are chosen. Point 1, 2 and 3 are in the inlet pipe and point 3, 4, and 5 from the outlet pipe of the snubber. For motor frequency 30, 40 and 50 Hz, data were collected and plotted and found these curve form. It shows that pressure drop at points 1, 2, 3 are similar fashion but different in slope for all the motor frequency setting. At the outlet part of the

snubber have also alike fashion of pressure gradient as inlet parts but with less slope for each pressure line. When motor frequency is set at 30Hz, the pressure at point 1, 2, 3, 4, 5 and 6 are 103.488, 103.181, 102.838, 101.850, 101.528 and 101.326 kPa, respectively. The pressure drop between point 3 and 4 for each motor frequency is more than the other measuring points due to the main body of snubber. For higher motor frequency, the pressure reduction rate is also higher. The pressure at point 3 and 4 for 30, 40, 50 Hz motor frequency are 102.838, 101.850; 103.732, 102.142 and 104.394, 102.342 kPa, respectively. The pressure gradient for motor frequency 50 Hz is the highest and lowest gradient is found at 30 Hz motor frequency.

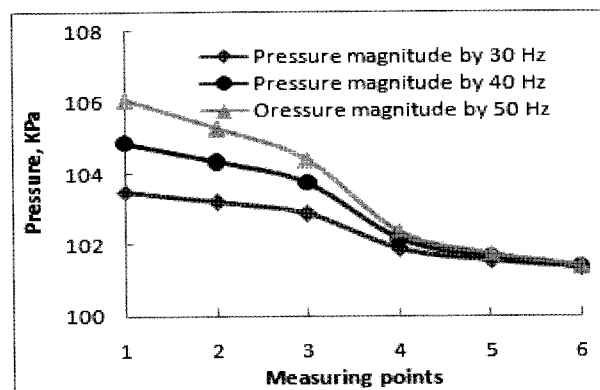


Fig. 5 Pressure magnitude distribution at different location for various motor frequency

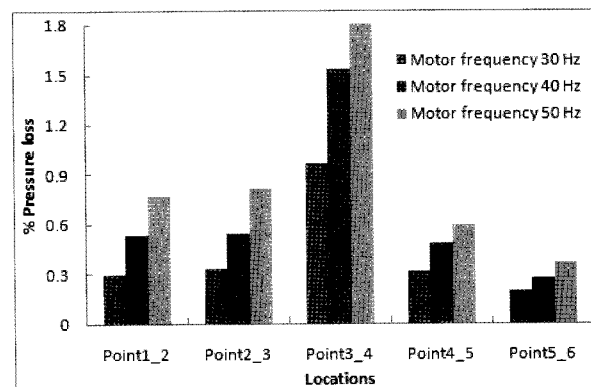


Fig. 6 Per cent pressure loss in snubber system

Fig. 6 shows percent pressure loss at different section of snubber system for 30, 40 and 50 Hz motor frequency. At point1\_2, Point2\_3, Point3\_4, Point 4\_5 and Point5\_6, the percentages of

pressure loss are 0.296, 0.530, 0.765; 0.333, 0.545, 0.812; 0.960, 1.533, 1.965 0.317, 0.482, 0.589 and 0.199, 0.275, 0.361%; respectively. It is found that positive correlation between motor frequency and per cent pressure loss exists. Similar trends were found by Akbar<sup>10)</sup>.

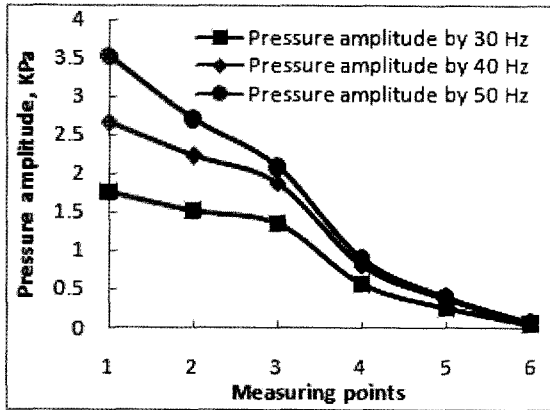


Fig. 7 Amplitude of pressure in snubber system

Amplitudes of pressures are plotted against their measuring points in snubber system and are presented in Fig. 7. Pressure amplitude in point 1, 2, 3 for motor frequency 30, 40, 50 Hz forms 3 different straight line having same slope for 30 and 40 Hz motor frequency and a more steep slope for 50 Hz motor frequency. After the main snubber body pressure amplitude are same trend as left side of snubber with lesser value. The maximum [1.756, 2.651, 3.518 kPa] and minimum [0.055, 0.075, 0.073 kPa] amplitudes are found at point 1 and 6, respectively, for all the motor frequency [30, 40, 50 Hz]. The snubber input and output amplitude [point 4] for motor frequency 30, 40, and 50 Hz are 1.349, 0.563; 1.881, 0.808 and 2.081, 0.898 kPa, respectively.

Table 1 Pressure amplitude reduction at snubber for various motor frequency

Motor frequency, (Hz)	Input amplitude, (kPa)	Output amplitude, (kPa)	Amplitude reduction (%)
30	1.349	0.563	58.249
40	1.881	0.808	57.026
50	2.081	0.898	56.871

### 3.2 Pressure variations inside the snubber

Computational fluid dynamics (CFD) can be applied to study pressure characteristics through the snubber. The boundary condition of CFD model was as in Fig. 8.

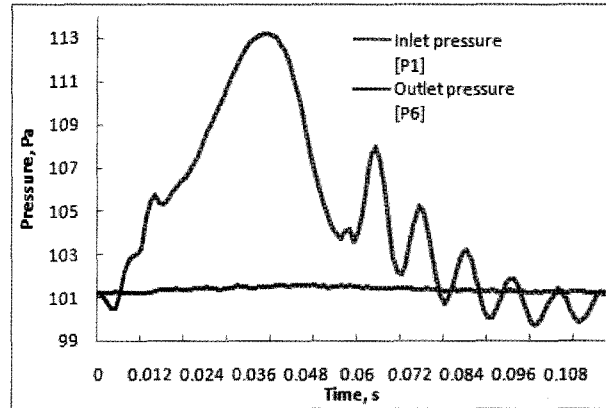


Fig. 8 Boundary condition of CFD simulation

To verify the CFD result with experimental result pressure at point 2 and point 5 are compared and found well matched (Fig. 9). In the Fig 10 the CFD simulation pressures and experimental pressures at point 3 and point 4 at the each side of main snubber body are shown. It is observed that there is a good agreement with CFD simulation results with experiment. So, the constructed CFD model can be used in describing pressure values in the snubber system. The pressure in the inlet pipe, inside the snubber including at buffer, and outlet pipe at each time step is given in Fig. 11 with different colours and numerical values for 40 Hz motor frequency. It forms a high pressure zone in the inlet pipe and below the buffer at the beginning. At the initial part of inlet pipe the pressure varies from 0.1125E+06 Pa to 0.1103E+06 Pa and then the pressure is reduced to 0.1081E+06 Pa and again it becomes 0.1059E+06 Pa at the end of inlet pipe. The pressure becomes to 0.1103E+06~0.1059E+06 Pa in the tube and having more pressure at buffer at same height of inlet pipe. At the beginning of the outlet pipe pressure is 0.1059E+06~0.1037E+06 Pa and it then reduces to 0.1015E+06 Pa at the end of it.

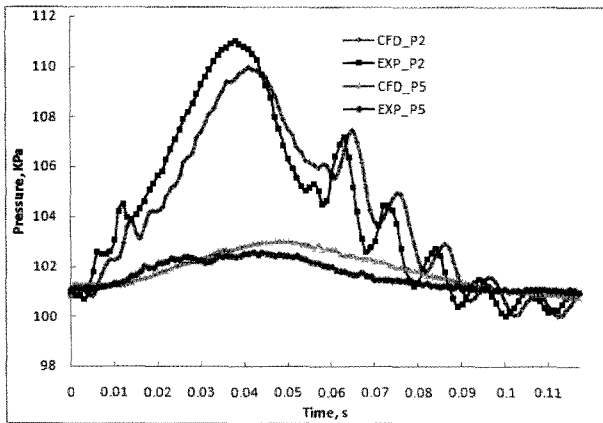


Fig. 9 Comparison of CFD simulated pressure with experimental pressure values at P2 and P5

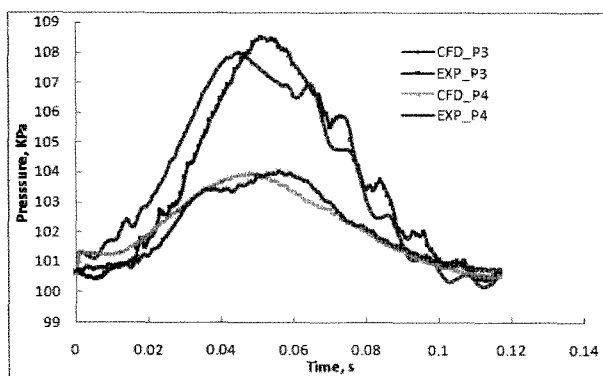


Fig. 10 Comparison of CFD simulated pressure with experimental pressure values at P3 and P4

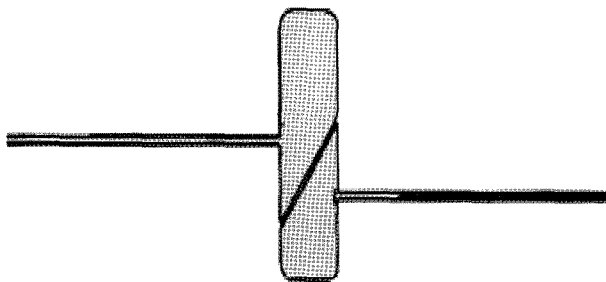


Fig. 11 CFD simulated pressure distribution inside the snubber

#### 4. Conclusion

More pulsation reduction and less pressure loss are expressed at the efficient the compressing system. In this research the findings are summarized as:

1. The pressure pulsation reductions by the acrylic snubber in hydrogen compression system

are 58.249%, 57.026% and 56.871% for motor frequency 30, 40 and 50 Hz, respectively.

2. In the snubber, the pressure loss 0.960%, 1.533% and 1.965% are accounted for motor frequency 30, 40 and 50 Hz, respectively.

3. At the different points in the snubber system CFD simulated pressure are compared with the experiment and ascertained as well matched. So, it can also be predicted the pressure at all points inside the main snubber body with both in numerical and graphical form. This CFD pressure values can be used to calculate the snubber performance in reciprocating hydrogen compression system.

#### Acknowledgement

This research was financially supported by the Human Resource Training Project for Regional Innovation from Ministry of Knowledge Economy and Korea Industrial Technology Foundation (KOTEF). The Authors would like to thank Region Strategic Planning Project from Ministry of Knowledge Economy and Brain Korea 21 Project.

#### Reference

1. J. Romm, 2004, "The car and fuel of the future: a technology and policy overview", The National Commission on Energy Policy by The Center for Energy and Climate Solutions, 2900 South Quincy Street, Suite 410, Arlington, VA 22206, USA.
2. [www.iea.org/Textbase/press/pressdetail.asp?PRESS\\_REL\\_ID=127](http://www.iea.org/Textbase/press/pressdetail.asp?PRESS_REL_ID=127)
3. S. A. Shayegan et al., 2006, "Analysis of the cost of the hydrogen structure for buses in London", *Journal of Power Sources*, 157(2), pp. 862~874.
4. M. A. Salvador, D. B. Gene, M. F. Joel, E. L. Francisco, 2006, "Vehicular storage of hydrogen in insulated pressure vessels", *International Journal of Hydrogen Energy* 31, pp. 2274~2283.

5. S. A. and I. E. Grossman, 2003, "A strategy for the integration of production planning and reactive scheduling in the optimization of hydrogen supply network", *Journal of Computers and Chemical Engineering*, Vol. 27, pp. 1831~1839.
6. V. V. Solovey, A. I. Ivanovsky, V. I. Kolosov, and Yu. F. Shmal'ko, 1995, "Series of Metal hydride high pressure hydrogen compressors", *Journal of Alloys and Compounds*, Vol. 231, pp. 903~906.
7. W. A. Akbar, K. J. Shim, and C. S. Yi, 2006, "Gas Pressure Fluctuation Characteristics inside Pipe Line Passing through a Snubber for Hydrogen Gas Compressor," *Proceeding of International Conference on Sustainable Energy Technologies*, Vicenza, Italy, 30 August - 1 September, 2006, pp. 659~664.
8. Origin Lab Co. 2003. Origin Reference v7.5. FFT Mathematical Description.
9. CD Adapco Group, 2004. Methodology Star CD Version 3.24.
10. W. A. Akbar, 2007, "A Study on high -pressured gas flow inside snubbers of reciprocating hydrogen compressor system", A MS thesis, Graduate School of Mechanical & Precision Engineering, Gyeongsang National University, South Korea, pp. 62~67.